JOURNAL OF MATERIALS SCIENCE **36** (2001) 4331–4343

Structural and compositional properties of sol-gel formed Ni, Co and Ni-Co oxide films

I. SEREBRENNIKOVA‡, V. I. BIRSS*
Department of Chemistry, University of Calgary, Calgary, AB, Canada T2N 1N4
E-mail: birss@ucalgary.ca

Sol-gel (SG) formed oxide films (between 60 and 800 nm in thickness) were deposited on Pt foil substrates by dip-coating from Ni, Co and mixed Ni-Co sols. After withdrawal at a constant rate, the films were dried at temperatures between 100 and 400°C for various periods of time (15 min to 1 hour). Electron diffraction and transmission electron microscopy studies have indicated that the as-formed SG films are nanocrystalline oxide materials, consisting of cubic units of NiO and/or CoO (and Co_3O_4, in pure Co SG films) in crystallites which are 1–4 nm in diameter, the size depending on the oxide composition and the drying conditions employed. Oxide films formed at 200°C are highly hydrous in nature, and drying at higher temperatures than this results in the loss of water, the formation of more compact films and an increase in the crystallite size. Based on the observed charge efficiencies (ca. 75% for pure Ni oxide and ca. 60% for 50:50 Ni:Co oxide films), it is suggested that only metal sites on the outer surfaces of the crystallites, with easy access to the solution ions and water, participate in the Ni-Co oxide redox reaction in alkaline solutions.

1. Introduction

Considerable interest in studying the structural and electrochemical properties of Ni, Co and mixed Ni-Co oxides has been driven by their many practical applications. Over the last few decades, numerous studies have been devoted to the better understanding of the redox reactions occurring during the cycling of Ni oxide electrodes, because of their use as the positive electrode in Ni/Cd, Ni/metal hydride and Ni/Fe batteries [1, 2]. Co oxide electrochemistry in alkaline solutions has been extensively studied due to its applications as an insertion cathode in Li batteries [3] and in electrochromic devices [4]. Both Co and mixed Ni-Co oxide materials, $Ni_xCo_yO_4$, have been investigated as promising catalysts for the oxygen evolution (OER) [5] and reduction (ORR) [6] reactions.

Ni and Co oxide/hydroxide films can be prepared by the anodic oxidation of metallic Ni (Co) substrates [7], by cathodic precipitation [8], electron-beam evaporation [9] and electrodeposition [10] methods. Chemical deposition [11], electrolytic deposition [12] and spray pyrolysis [13] methods have been utilized to make mixed Ni-Co oxide films, which can also be formed by the anodic oxidation of polycrystalline and amorphous Ni-Co alloys [14]. Since the 1980's, the sol-gel (SG) technique has become attractive to the electrochemical community as a convenient route to the formation of amorphous or crystalline xerogels, aerogels and conductive hydrous gels [15] of controlled composition. The applications include as sensors and modified electrodes [16], electrochromic devices [17], corrosion protection coatings [18], etc.

In the last several years, the SG synthesis of Ni and Co oxide materials has drawn considerable interest [19–32]. For example, Monaci *et al.* [30] prepared composite materials of Ni nanoparticles dispersed in a SiO_2 phase, and studied them by means of thermogravimetric analysis, transmission electron microscopy (TEM) and X-ray diffraction (XRD). They found that composites containing 7% Ni showed good catalytic activity towards the hydrogenation of toluene to form methylcyclohexane. High surface area SG-derived films consisting of nanosized NiO/Ni particles have been found by Liu *et al.* [22] to be good electrochemical capacitors. TEM and XRD studies indicated that samples prepared from dilute sols have smooth surfaces and consist of tightly packed arrays of small particles (ca. 10 nm in diameter). The use of concentrated sols resulted in the formation of larger particles (100 to 120 nm in diameter), which agglomerated during gelation, yielding rough surfaces with high surface areas [22] The pseudocapacitance arising from the rapid Ni(II)/(III) redox reaction, combined with the large double layer capacitance of these high surface area films, resulted in a very high capacitance of these composite materials.

* Author to whom all correspondence should be addressed.
‡*Present Address*: Department of Chemistry, University of Utah, Salt Lake City, UT 84112, USA.

El Baydi and coworkers prepared powders of $LaNiO_3$, $NiCo_2O_4$ [31] and Co_3O_4 [25] via the SG route and characterized them by thermogravimetric analysis, scanning electron microscopy (SEM), IR spectroscopy, XRD and cyclic voltammetry (CV). Propionic acid precursors were found to yield high surface area powders (20 to 55 m^2/g) at low temperatures of preparation, especially in the case of $NiCo_2O_4$ (250–300°C). For $LaNiO_3$, malic acid precursors have been found to be more advantageous, allowing lower preparation temperatures to be employed, vs. via the propionic acid route (600 vs. 750°C, respectively). High roughness factors (30–1500), estimated from the CVs, make these materials good candidates as electrocatalysts for the OER.

Our research has been focused on the structural and electrochemical properties of SG derived Ni, Co and mixed Ni-Co oxide films [19–34], studied by the use of a combination of electrochemical and surface analytical techniques. One of the objectives of the present work has been to gain knowledge about the structure and composition of the SG formed Ni-Co oxide films and to then correlate these physical/chemical properties with their electrochemical behavior. Energy dispersive X-ray fluorescence (EDX), and X-ray and electron diffraction (XRD/ED) techniques were used in order to determine the SG oxide film composition. TEM, SEM and field emission SEM (FESEM) studies were carried out to obtain the film thickness and other nanostructural information.

2. Experimental

2.1. Preparation of SG films

The Ni, Co and mixed Ni-Co sols were prepared as described elsewhere [35]. The SG films were deposited on Pt foil substrates by a dip-coating procedure, in which the substrate was immersed into the sol and withdrawn at a constant rate between 1 and 60 cm/min to control the film thickness. The surface films gelled during solvent evaporation. Following this, the SG-coated substrates were heated in air in an oven (Fisher 116G) or furnace (Barber-Colman, Thermolyne Corp.) at temperatures between 100 and 400°C for 15 to 60 min to produce compact films, subsequently studied by the techniques described below.

2.2. Scanning (SEM), field emission (FESEM) electron microscopy and energy dispersive X-ray fluorescence (EDX) analysis

SEM, FESEM and EDX techniques were employed in order to determine the SG oxide film thickness and composition. A Hitachi 100 SEM (Health Sciences Center, University of Calgary) and a Cambridge S250 Stereoscan SEM system (Department of Geology and Geophysics, University of Calgary), the latter coupled to a Kevex 7000 Micro-X probe, were employed for the SEM and semi-quantitative EDX work, respectively. 99.9% purity Ni foil (Aldrich) and Co wire (Aldrich) specimens were used as calibration standards for the EDX measurements. For both the SEM and EDX studies, an accelerating voltage of 20 kV, a typical working distance of 15 mm and a data acquisition time of 60 sec (EDX work) were generally employed. A standard sample (2160 lines/mm) was used for accurate dimensional measurements by SEM. A Hitachi S-4500 FESEM (Surface Science Western, University of Western Ontario) was used to obtain high resolution morphological information. An accelerating voltage of 5 kV and a working distance of 6 mm were used. The SG oxide films for FE-SEM studies were dip-coated on Pt foil substrates, dried in an oven and, after their CV response in 1 M NaOH was recorded, the samples were sent for FESEM analysis.

SG coated Pt foil substrates, employed in SEM studies, were often bent mechanically in order to fracture the SG films, enabling an easier determination of their thickness. The samples were attached to Al stubs using conducting carbon tape (E. T. Enterprises). Before being placed in the chamber, samples were sputter-coated with a ca. 30 nm thick Au/Pd film to reduce charging effects during the SEM examination.

2.3. Transmission electron microscopy (TEM) and electron diffraction (ED) studies

TEM and ED measurements were employed in this work to obtain nanostructural and compositional information about the SG oxide films. The SG oxide samples were formed by dip-coating copper grids (G400, JBS EM and G1000HS-C3, Gilder) in the sol and then drying, according to the procedures described above. A Hitachi H-7000 TEM (Health Sciences Center, University of Calgary) was employed in all of this work. The electron diffraction spectra were obtained at a 100 kV accelerating voltage (wavelength of diffracted electrons was 0.037 Å).

2.4. X-ray diffraction (XRD)

X-ray diffraction studies were carried out in order to determine the structure and composition of the SG-formed oxide films. Films were dip-coated on glass slides or Pt foils and dried in an oven at controlled temperatures for 15 min. XRD measurements were performed employing a 2000 Philips Scintag Diffractometer (Department of Geology and Geophysics, University of Calgary). Cu K_α radiation was used as the X-ray source ($\lambda = 1.542$ Å).

2.5. Electrochemical studies

The electrochemical experiments were carried out using an EG&G PARC 173 potentiostat/galvanostat (with an add-on PARC 179 digital coulometer), coupled with an EG&G 175 programmer. The voltammetric response was plotted on a Hewlett-Packard 7044B X-Y recorder. A high area Pt mesh electrode served as the counter electrode (CE), while a reversible hydrogen electrode

(RHE) was employed as the reference electrode (RE) in all of this work.

The equilibrium charge density of the SG oxide films was determined by integrating the cathodic peak, at a slow sweep rate of 5–10 mV/s, between 1.0 and 1.55 V *vs*. RHE. The double layer current of the underlying Pt substrate was used as the baseline for the integration.

2.6. Experimental determination of charge efficiency of SG oxide films

The charge efficiency of the SG oxide films was determined by combining the CV data with the subsequent analysis of the metal content of the film, after dissolution, by inductively coupled plasma–atomic emission spectroscopy (ICP). For the ICP studies, SG oxide films of a range of different compositions were formed on Pt foil substrates (0.3 to 0.7 cm^2), employing a withdrawal rate of 6 cm/min and drying at 200°C for 15 minutes. The equilibrium cathodic charge densities were determined by integrating the slow sweep rate CVs between 1.55 and 1.0 V vs. RHE. Following this, the SG oxide films were stripped from the Pt substrates by sonicating in 2.5 ml of 0.1 M HNO_3 overnight. The volume of the sample solutions was then brought to 25 ml with distilled water. 1,000 ppm ICP grade solutions of Ni and Co (Ultra Scientific) were used to prepare the 40 ppm Ni and Co standards used for calibration. The analysis of the Ni and Co content of the sample solutions was performed (using emission lines at 216.5 nm for Ni and 228.6 nm for Co) on a Thermo Jarrel-Ash AtomScan 16 ICP-AES spectrometer.

3. Results and discussion

3.1. SEM, FESEM and EDX studies of SG oxide films

3.1.1. Film composition and morphology

The EDX measurements confirmed the presence of Ni and Co in the SG-derived Ni and Co oxide films, respectively. A semi-quantitative analysis of the EDX spectrum of a typical 50:50 Ni-Co SG oxide film (Fig. 1), coated on a Pt substrate from an equimolar (0.23 M each) Ni-Co sol, yielded a ca. 1:1 ratio of Co to Ni in the film, as anticipated. The fact that the Pt signal is so large (Fig. 1) indicates that the thickness of the SG oxide films formed on the Pt substrate is substantially less than a micron, the depth of penetration of the 20 keV electrons.

SEM and FESEM studies were performed in order to obtain structural information about the film and to determine the SG film thickness. Fig. 2 shows a SEM image of a 50:50 Ni-Co SG oxide film, formed by dip-coating a Pt substrate at a withdrawal rate of 24 cm/min and then drying at 200°C for 15 min. The "mud-cracked" structure is typical for hydrous oxide films [22], and likely arises from the dehydration of SG oxide caused by exposure to vacuum in the SEM chamber. All SG films under study appeared very stable to the vacuum and no curling or flaking of edges of the film was observed during SEM examination.

FESEM images (Fig. 3) were obtained of various SG oxide films, prepared on Pt substrates, in order to obtain structural information on a smaller scale. These films were formed at a withdrawal rate of 6 cm/min, followed by drying at 200°C for 15 min. In regions

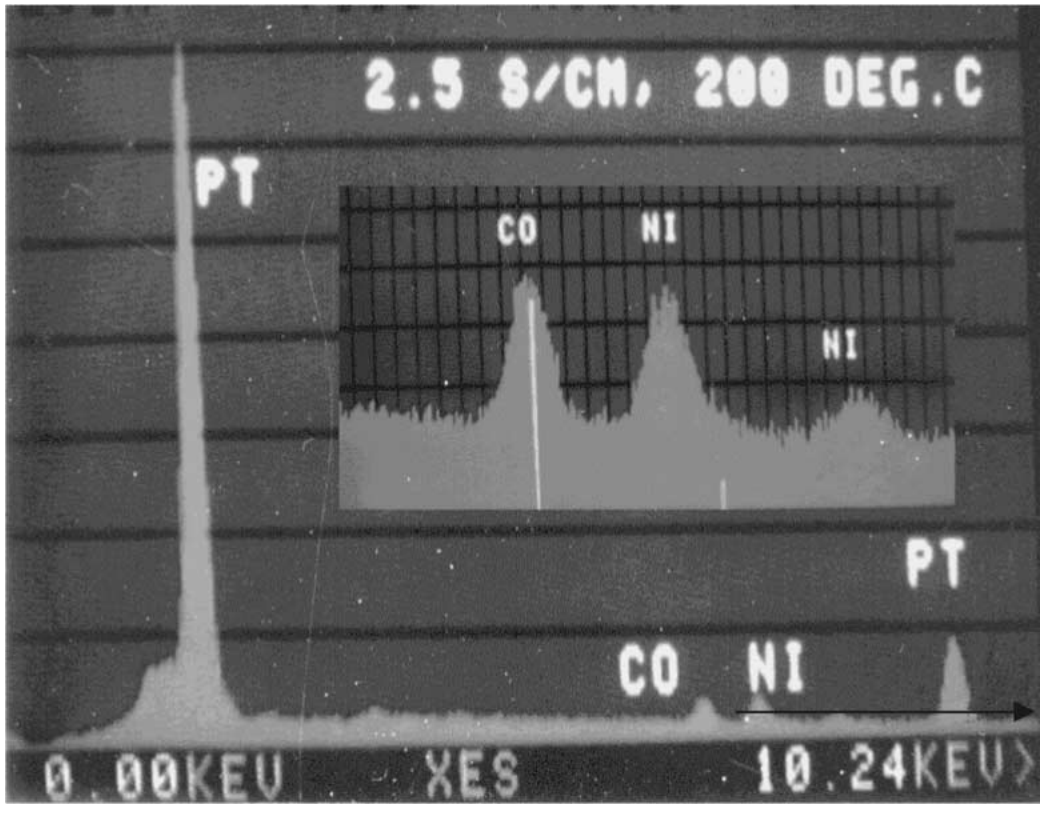

Figure 1 EDX spectrum of a 50:50 Ni-Co SG oxide film on a Pt substrate. Film formed at a withdrawal rate of 24 cm/min and dried at 200°C for 15 min.

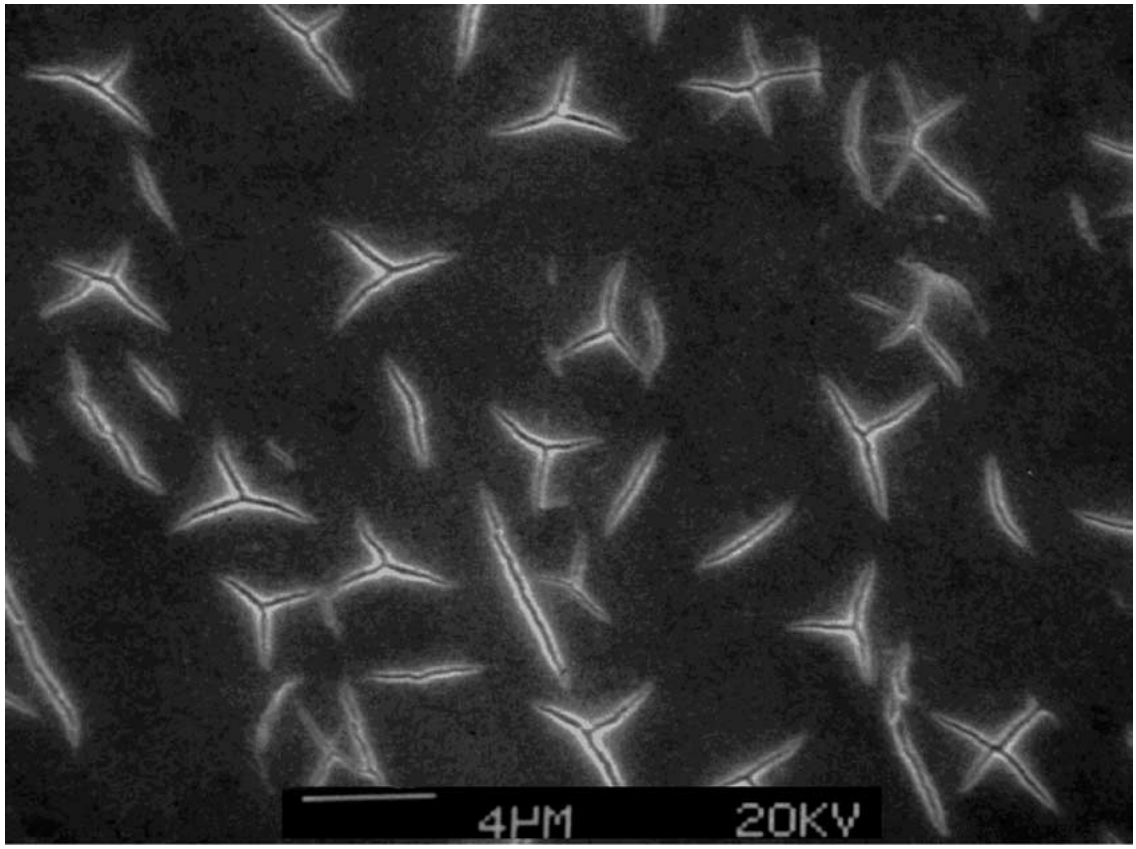

Figure 2 SEM image of a 50:50 Ni-Co oxide film, formed on Pt substrate at a withdrawal rate of 24 cm/min and dried at 200°C for 15 min.

adjacent to the cracks, the surface of a 50:50 Ni-Co oxide film (Fig. 3a) can be seen to be relatively smooth at high magnification, showing fine grains, ca. 10 nm in size. In contrast, the surface of a SG formed Co oxide film (Fig. 3b) has a more granular structure, containing flake-like particles ca. 30–70 nm in size. FE-SEM images of SG-formed Ni oxide films (not shown) are very similar to those seen for 50:50 Ni-Co films. It will be seen below that there is a good correlation between the size of the oxide film particles and the electrochemical charge density, obtained from CV experiments.

3.1.2. Effect of the substrate withdrawal rate from the coating solution

The rate at which a substrate is withdrawn from the SG coating solution determines the thickness of the film, due to the competition between several forces, i.e., viscous drag upwards on the liquid by the moving substrate, the force of gravity and surface tension of the concave sol meniscus [36]. It is predicted that the use of a more rapid substrate withdrawal rate from a SG solution leads to the deposition of thicker films than when a slow withdrawal rate is used [36].

The SEM results support this prediction. When 50:50 Ni-Co SG oxide films were formed at a withdrawal rate of 24 cm/min and dried at 200°C for 15 min., the average thickness was found to be ca. 800 nm, as can be seen from a micrograph of a mechanically fractured SG oxide film of this kind in Fig. 4a. The use of the same drying treatment, but a slower withdrawal rate of 6 cm/min, yields films with thicknesses of ca. 400 nm (Fig. 4b). For the pure Ni SG oxide films, similar film thicknesses have been obtained as a function of the drying temperature.

In the case of pure Co oxide films, a significant scatter in the measured film thickness has been observed, e.g., for films formed at 6 cm/min and dried at 200°C, film thickness ranged between 200 and 500 nm. All Co oxide SG films display a much greater sensitivity towards preparation conditions, reflected both by their structural (film thickness and oxidation state) and electrochemical (stability and charge density) properties [37], as compared to pure Ni and mixed Ni-Co SG oxide films.

3.1.3. Impact of the drying treatment as seen by SEM

It is known that the conditions used for film drying should greatly affect the density of SG-derived coatings, with the film shrinking in the direction perpendicular to the substrate as the solvent evaporates [36]. Heat treatment during the preparation of SG films results in the loss of water of hydration and organic residues, as was indicated by our IR spectroscopy results [19], as well as in the overall shrinkage of the film. Thus, when the substrate is withdrawn at a constant rate from the same solution, thinner coatings are expected after drying at higher temperatures.

The impact of the drying temperature on the thickness of typical SG films under study is illustrated in SEM images of mechanically fractured SG oxide films (Figs 4 and 5) and summarized in Table I.

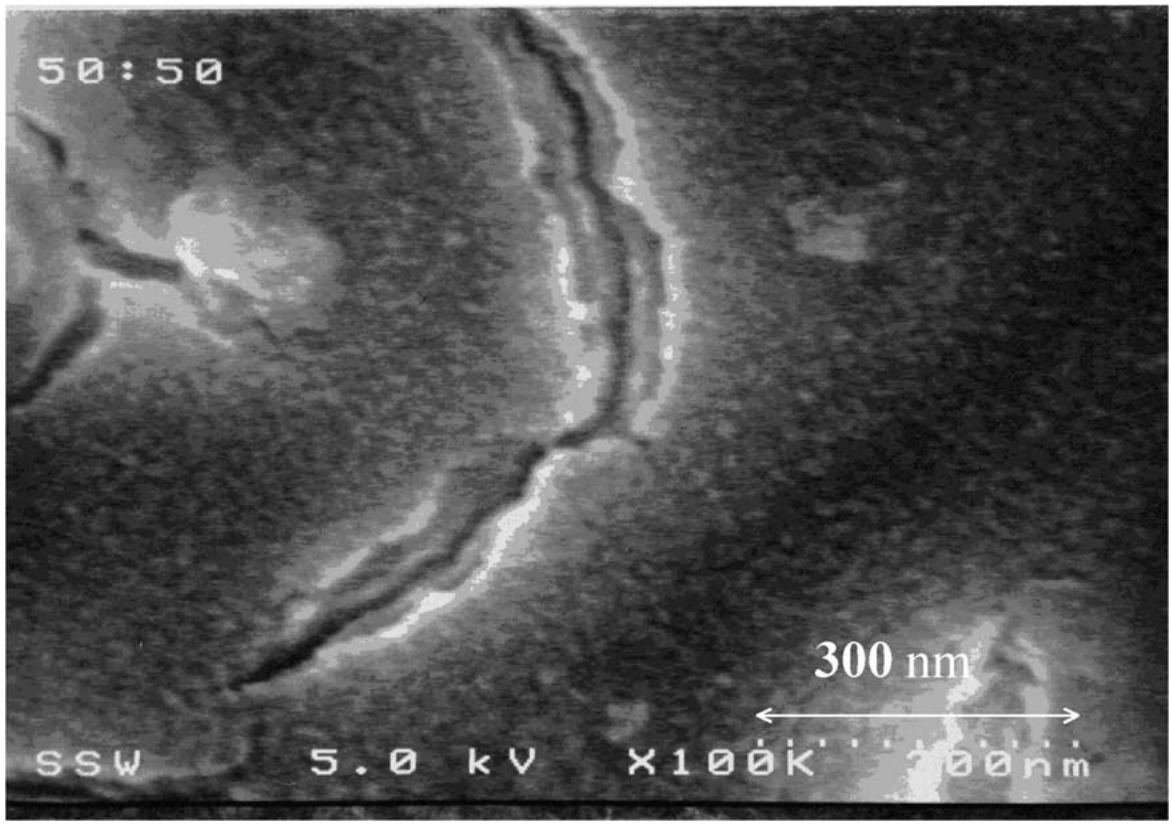

(a)

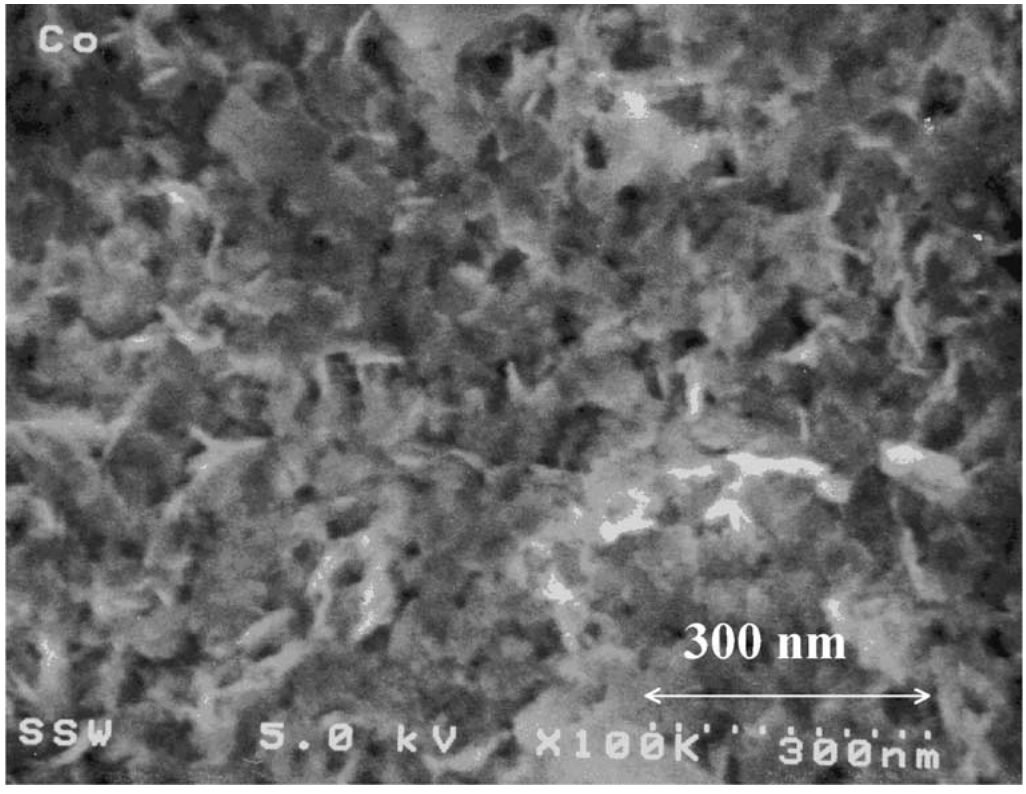

(b)

Figure 3 FESEM image of a 50:50 Ni-Co (a) and Co (b) SG oxide films on Pt substrate. Films prepared at 6 cm/min withdrawal rate and heated at 200°C for 15 min.

For films formed under otherwise identical conditions (24 cm/min withdrawal rate, 15 min drying time), an increase in the drying temperature from 200°C (Fig. 4a) to 400°C (Fig. 5) results in the formation of a more compact film, with the film thickness decreasing from 800 to ca. 130 nm. There is less known about the effect of drying time on the thickness and properties of SG formed oxide films. However, our data show that the thickness of 50:50 Ni-Co oxide films, formed at a withdrawal rate of 6 cm/min, decreases from 400 nm

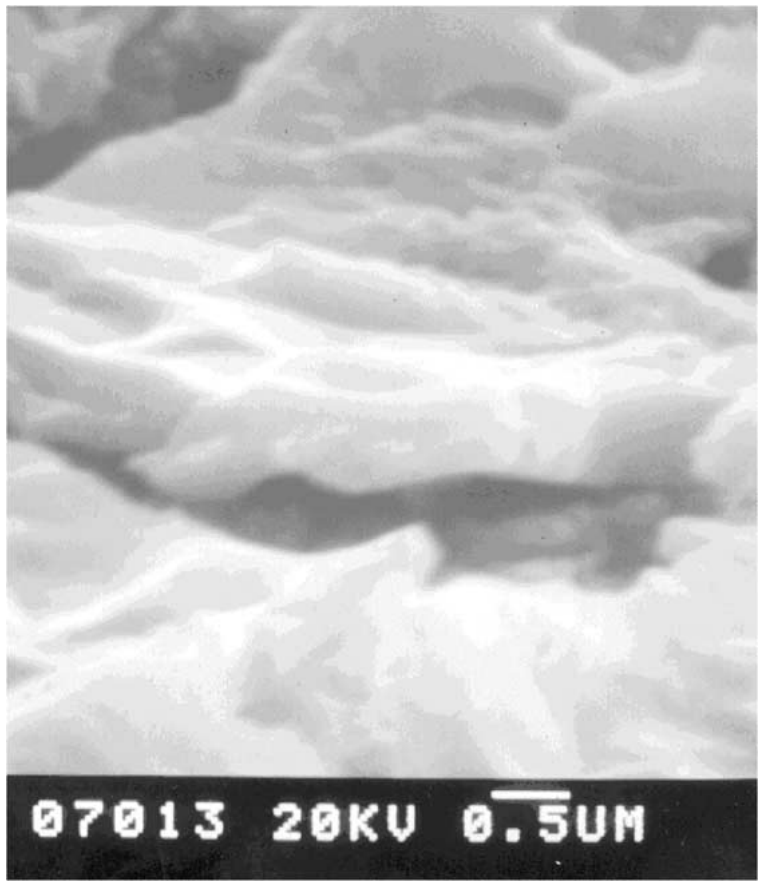

(a)

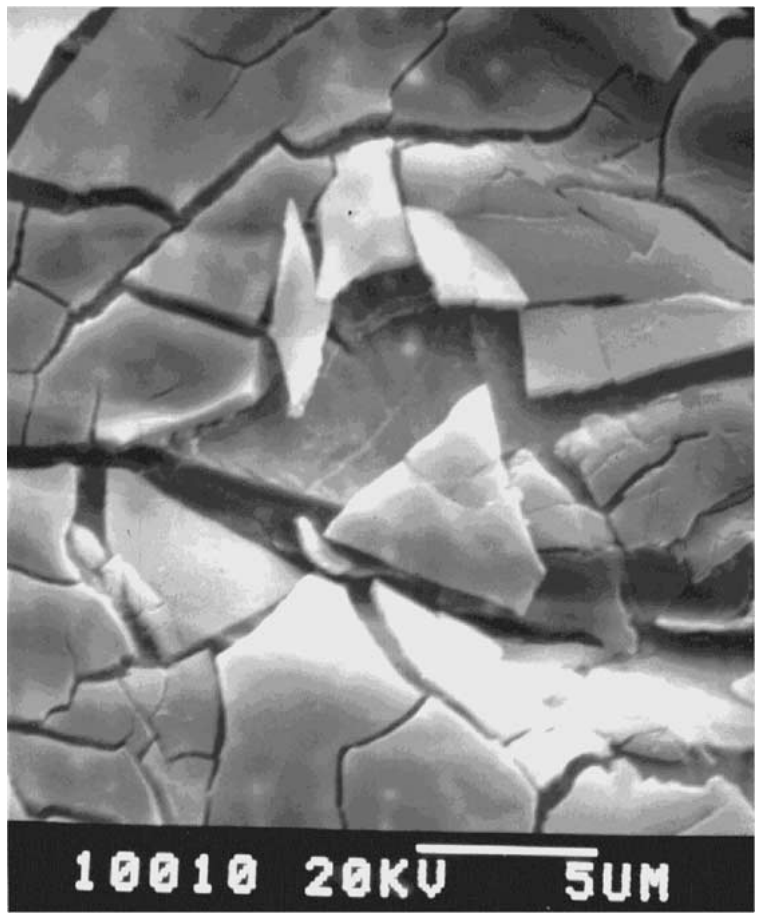

(b)

Figure 4 SEM image of the mechanically fractured 50:50 Ni-Co SG oxide films on a Pt substrate. Films formed at 24 (a) and 6 cm/min (b) and dried at 200°C for 15 min.

(a)

(b)

Figure 5 SEM image of a mechanically fractured 50:50 Ni-Co SG oxide film on a Pt substrate. Film formed at a withdrawal rate of 24 cm/min and dried for 15 min at 400°C. SEM of the film at a higher magnification is shown in (b).

TABLE I The impact of SG formation conditions on the thickness of 50:50 Ni-Co oxide films

Withdrawal rate (cm/min)	Drying temperature (°C)	Drying time	Film thickness (nm)
24	200	15 min.	800
6	200	15 min.	400
6	400	15 min.	130
6	250	1 hour	65

(200°C, 15 min) to ca. 65 nm (250°C, 1 hour) when the film undergoes a more extensive (higher temperature, longer time) drying treatment (Table I).

3.2. TEM, X-ray and electron diffraction studies of SG oxide films

X-ray diffraction (XRD) was employed in order to establish the compositional properties of these SG oxide films. The broad peaks observed in the XRD patterns did not allow us to establish the composition (oxide vs. hydroxide, oxidation state, etc.) of these SG films. Normally, amorphous solids show a diffuse "halo", indicating that, although randomly arranged, on average, the atoms are similar distances apart. However, very small crystals may cause scattering of X-rays to occur at angles near the Bragg angles [38]. This results in the broadening of the diffracted beam and materials display an "amorphous" halo pattern. As beam broadening is directly proportional to the wavelength [38], electron diffraction using smaller wavelengths could be employed to obtain structural information about nanocrystalline materials.

Therefore, the crystal structures of the SG formed materials were determined by means of electron diffraction studies, employing high energy electrons with a wavelength of 0.037 Å. The experimental data were compared with the JCPDS—International Center for Diffraction Data files (Table II). Based on the results shown in Table II, it was concluded that all of the investigated SG films are oxide materials, independent of the heating temperature or time. In the case of the Ni SG oxide films, it was difficult to distinguish between the cubic and rhombohedral NiO structures. It should be pointed out that, in the case of pure Co SG films, d-spacings characteristic for both cubic CoO and Co_2O_3 are observed and the lines are found to fit the spinel Co_3O_4 structure, indicating the presence of both Co(II) and Co(III) states in these films. In contrast, Co in the 50:50 Ni-Co films is found to be only in the Co(II) state, so these materials have been indexed as a mixture of cubic NiO and CoO.

The nanocrystalline nature of these SG oxide films was confirmed by the results of the TEM studies. The TEM micrographs of all SG oxide films under study show the presence of nanometer-sized grains. Typical TEM images and ED patterns of 50:50 Ni-Co and Co SG oxide films, formed at various temperatures, are shown in Figs 6 and 7, respectively. The films are composed of small nanocrystallites, ranging in diameter from 0.5 to 3 nm. If formed using an identical drying treatment (e.g., 200°C for 15 min), the average grain size increases in the following sequence: pure Ni SG oxide film (ca. 1 nm) < 50:50 Ni-Co oxide (ca. 1.3 nm) < pure Co oxide film (ca. 1.5 nm).

From the results of the TEM studies, it is concluded that all of the as-formed SG films under study can be described as nanocrystalline oxide materials. The ED results show that they consist of cubic units of NiO and/or CoO (or a $CoO{\cdot}Co_2O_3$ mixture, in the case of pure Co SG films). The cubic oxide units cluster together to form crystallites ranging from 0.5 to 4 nm in size, depending on the oxide composition and drying conditions. The SG oxide films under study can be viewed as a continuous network of interconnected nanosized particles.

TABLE II Interplanar *d*-spacings (Å) of the most intense rings from the ED studies of SG films

SG film composition	Formation temperature (°C)	Experimental *d*-spacing (Å)	Proposed structure	Reference
Ni	190	2.4	NiO (cubic)	[39, 40]
		2.07		
		1.47	NiO (rhomb)	[41]
Co	190	2.86	$CoO{\cdot}Co_2O_3$	[42]
		2.41	(cubic)	
		2.00		
		1.54		
		1.43		
		1.20		
50:50 Ni-Co	190	2.61	CoO (cubic)	[43]
		2.41	NiO (cubic)	[39, 44]
		2.07	NiO (rhomb)	[41]
		1.50		
		1.43		
		1.31		
Ni	300	2.4	NiO (cubic)	[40, 44]
		2.07	NiO (rhomb)	[45]
		1.50		
		1.23		
Co	300	4.3	$CoO{\cdot}Co_2O_3$ (cubic)	[42]
		2.86	Co_3O_4 (cubic)	[46]
		2.41		
		2.00		
		1.54		
		1.40		
		1.20		
50:50 Ni-Co	300	2.41	CoO (cubic)	[47]
		2.07	NiO (cubic)	[48]
		1.47		
		1.23		
		1.03		
Ni	400	2.41	NiO (cubic)	[40, 44]
		2.07	NiO (rhomb)	[45]
		1.47		
		1.20		
		1.02		
Co	400	4.63	Co_3O_4 (cubic)	[49, 50]
		2.86		
		2.41		
		2.07		
		1.67		
		1.43		
50:50 Ni-Co	400	2.41	NiO (cubic)	[48]
		2.07	CoO (cubic)	[47]
		1.47		
		1.20		
		1.02		

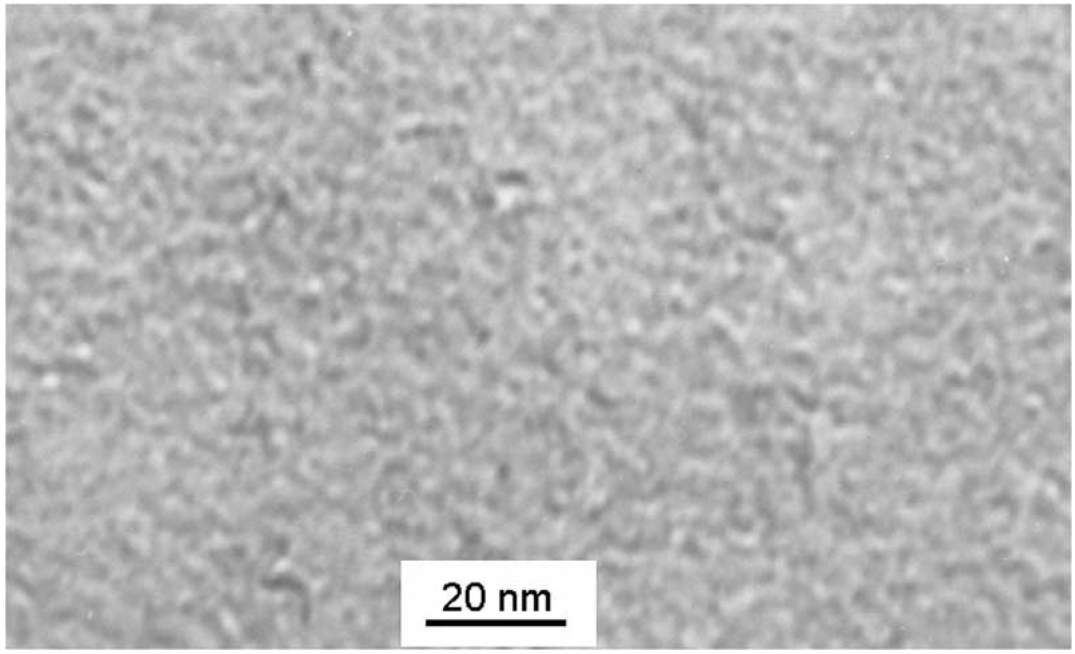

(a)

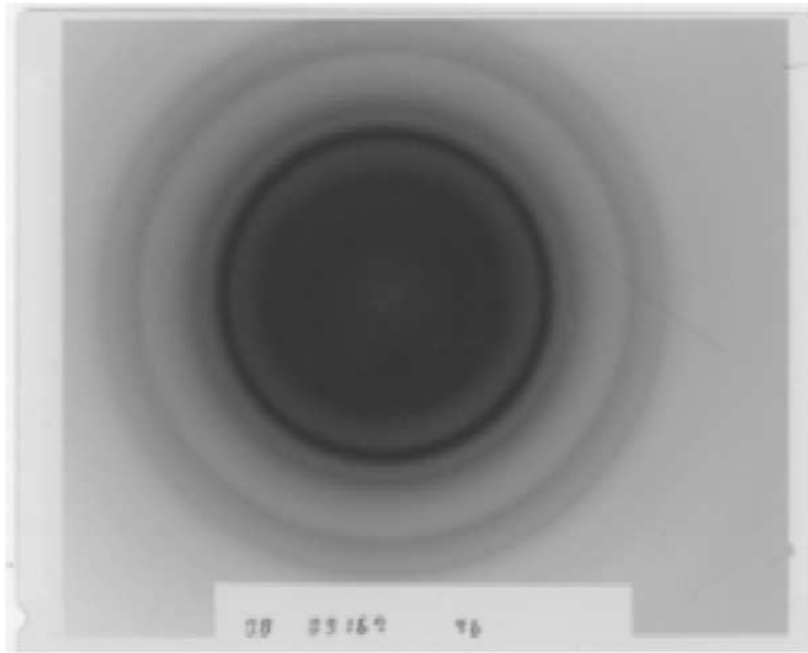

(b)

Figure 6 TEM image (a) and ED pattern (b) of a 50:50 Ni-Co oxide film formed on a Cu grid at a withdrawal rate of 2.4 cm/min and dried at 200°C for 15 min.

The SG drying temperature strongly affects the SG film structure. The use of higher temperatures during the drying of the films yields an increased intensity of the diffraction lines. This would suggest that larger crystals are formed. Larger crystallite sizes would also lead to a reduction in the fraction of "amorphous" boundaries between the crystallites [51], so that the SG oxides appear to be more crystalline in nature when dried at 300 and 400°C than at lower temperatures. TEM data indicated that an increase in the drying temperature from 200 to 300°C results in an increase in the crystallite size, e.g., from 0.5–1.5 nm to 2–4 nm for pure Co SG oxide films. In addition, higher drying temperatures not only yield larger crystallite sizes, but may also cause sintering of the crystallites, which was observed also for pure Co SG oxide films. The TEM image of the Co SG oxide dried at 300°C shows clusters of crystals approximately 70–100 nm in size (Fig. 7b). These results are in agreement with the FESEM studies, as well as with prior literature data [52, 53].

The temperature employed during drying of the SG oxide films under study has a marked effect on the microstructure of the films and, as a consequence, on their electrochemical response. Fig. 8 shows the CVs of two 50:50 Ni-Co SG oxide films, formed under otherwise identical conditions, but dried at 200 and 300°C. While the CV shape remains basically unchanged, films dried at 300°C display a pronounced decrease in the charge

density. It should be noted that the experimental sweep rate was sufficiently slow in both of these experiments such that it can be assumed that all of the active metal sites in the film were being oxidized/reduced. It has been found in our work that films formed at temperatures between 180 and 250°C, but otherwise formed identically, display the maximum charge capacity [19]. The observed decrease in the charge density of the SG films formed at temperatures above 250°C must result from the collapse of the film structure (film shrinkage seen by SEM) and the increased crystallite size (TEM data) and, thus, a reduced surface area.

3.3. The theoretical charge efficiency of the SG oxide films

In order to estimate the theoretical charge efficiency of the SG oxide films, defined as the ratio of active metal

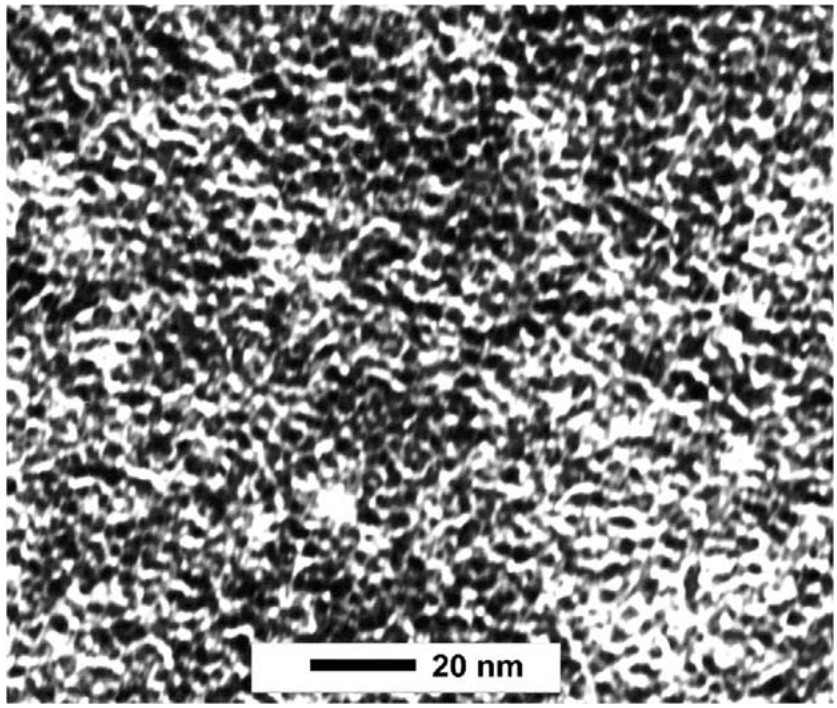

(a)

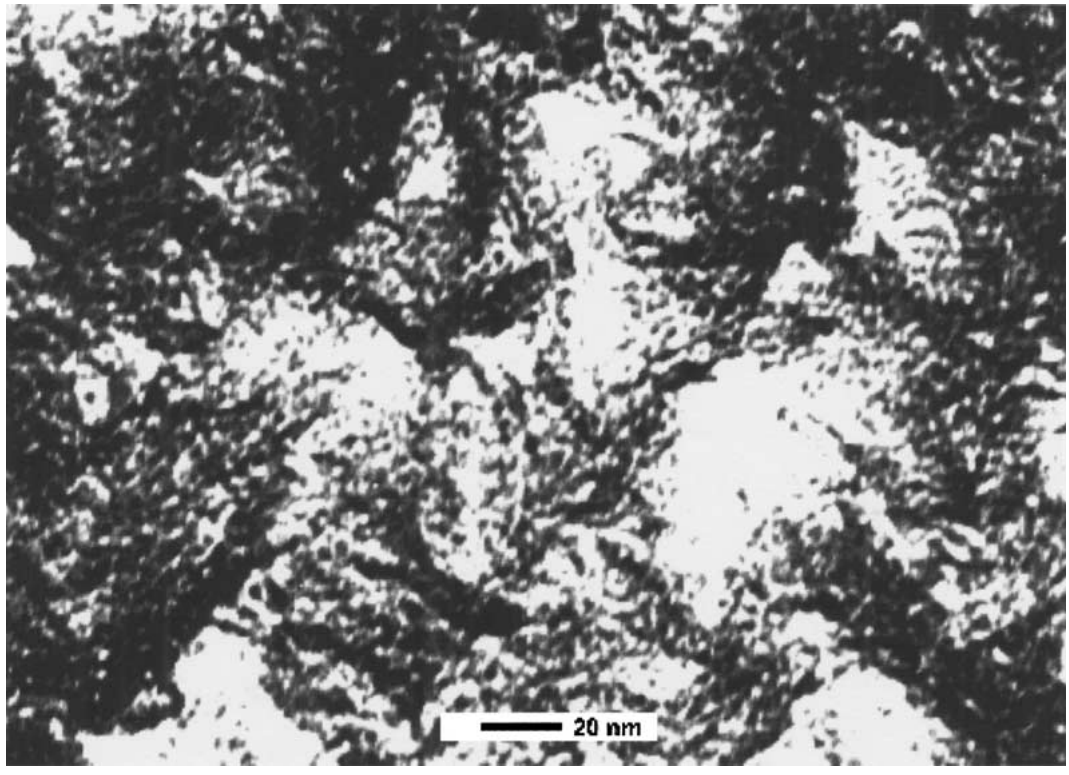

(b)

Figure 7 TEM image (a-b) and ED pattern (c) of a Co oxide film formed on a Cu grid at a withdrawal rate of 2.4 cm/min and dried at 300°C for 15 min. (*Continued*.)

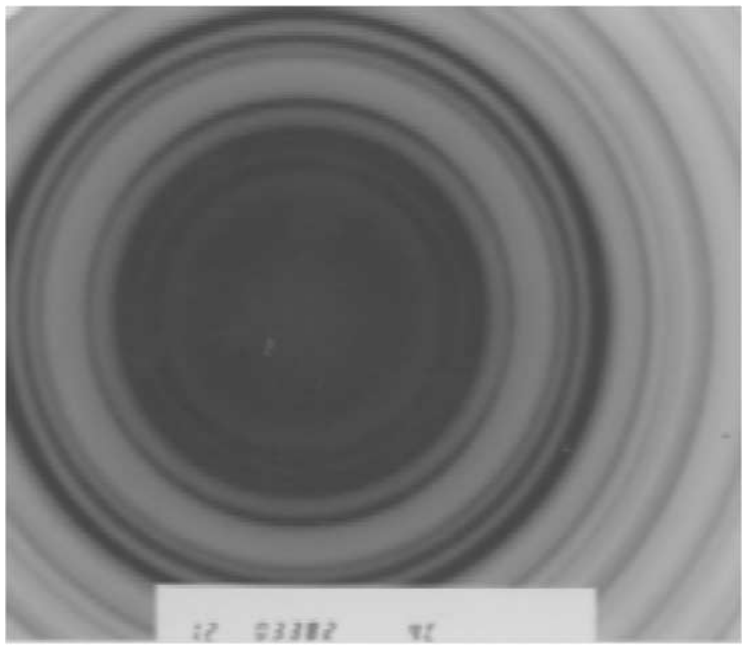

(c)

Figure 7 (*Continued.*)

(Ni, Co) sites that participate in the redox reaction to the total number of metal atoms, the following analysis has been carried out. Fig. 9 shows a unit cell of cubic Ni oxide (fcc), with a lattice constant of 0.42 nm [40]. Assuming an average crystallite size of a SG formed Ni oxide film, dried at 200°C for 15 min, to be ca. 1 nm (TEM data), each NiO crystallite would contain 8 unit cells. The total number of Ni sites in a single crystallite of this size has been calculated to be 62, with 48 Ni atoms (or ca. 77% of total Ni sites) occupying outer surface sites. The surface to volume ratio of the nanocrystalline Ni SG oxide films is therefore quite high, predicting a charge efficiency in the range of 75–80%.

50:50 Ni-Co SG oxide films, formed at 200°C for 15 min, consist of a mixture of fcc NiO and CoO (Table I). It is suggested that the Co atoms replace every other Ni atom in the unit cell, with a lattice parameter of 0.42 nm [40, 47]. The average crystallite size for these films, as determined from the TEM results, is ca. 1.3 nm. Thus, each crystal is composed of 27 unit cells. If, according to prior literature reports [1], only Ni is electrochemically active, the total number of Ni sites is 90, with the number of surface Ni sites then being 54, yielding a charge efficiency of ca. 60%. This treatment would predict that ca. 60% of the available Ni atoms in the 50:50 Ni-Co SG oxide film would participate in the redox reaction. If both Ni and Co sites participate in the electrochemical Ni(Co)(II)/(III) reaction, the overall charge efficiency, defined as the ratio of surface sites (both Co and Ni, which is equal to 108) to the total number of metal atoms (171), is also expected to be ca. 60%.

In the case of pure Co SG oxide films, dried at 200°C for 15 min. and having an fcc structure (Table I) with a lattice parameter of ca. 0.81 nm [42], a 1.5 nm crystallite would contain 8 unit cells. The theoretical charge efficiency is expected to be the same as in the case of pure Ni SG oxide films, i.e., 77%.

For comparison, the experimental charge efficiency was determined by means of CV and inductively coupled plasma (ICP) spectroscopy. In the CV experiment,

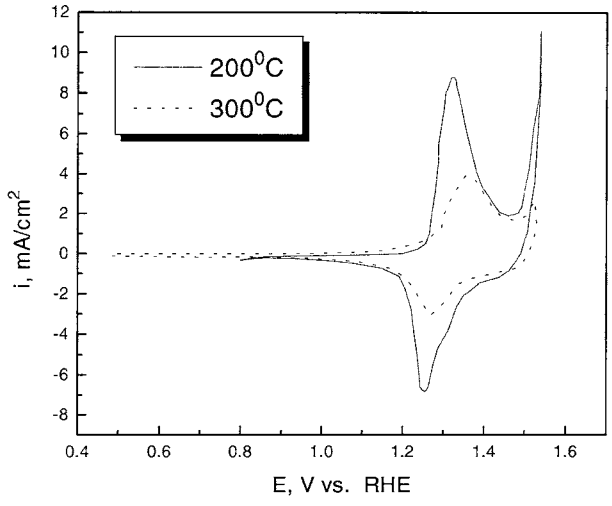

Figure 8 CVs ($s = 20$ mV/s) of 50:50 Ni-Co SG oxide films in 1 M NaOH. Films formed on Pt foil substrates (0.5–0.8 cm^2) at a withdrawal rate of 6 cm/min and dried at 200 (solid line) and 300°C (dotted line) for 15 min.

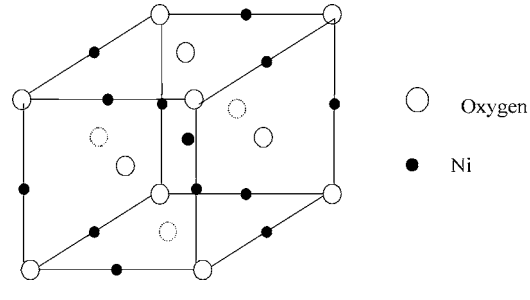

Figure 9 A unit cell of the fcc Ni SG oxide.

the charge density was obtained by integrating the cathodic peak between 1.0 and 1.5 V (see Fig. 8) at a sufficiently slow sweep rate, such that all of the metal sites are reacting. The SG films were then dissolved in acid and the Ni and Co content in the analyte was then determined by means of ICP spectroscopy. Assuming that only Ni is electrochemically active [1] and that each Ni site contributes one electron [1] in the Ni(III)/(II) redox reaction, the theoretical charge density was calculated for each sample. In the case of pure Co SG oxide films, a 2 electron/Co site ratio has been used to account for the expected [54] Co(IV)/(III) and Co(III)/(II) transitions over this potential range. Taking the ratio of the experimental charge density (from the CVs) to the theoretical one (from ICP), the experimental charge efficiency was calculated for each of the SG oxide films.

This procedure led to a charge efficiency of ca. 50–60% for both pure Ni and 50:50 Ni-Co SG oxide films and only 5–9% for the pure Co oxide films [33]. The good agreement between theoretical and experimental values of the charge efficiency for pure Ni and 50:50 Ni-Co SG oxide films confirms our suggestion that only metal sites on the outer surfaces of the crystallites participate in the redox reaction, in agreement with some prior literature reports [9]. The hydrated metal cations (Na^+) and OH^-, required to maintain electroneutrality within the film during the $Ni(Co)^{2+/3+}$ redox reaction [8], must then move in the channels between the SG oxide particles. A more detailed comparison of the theoretical charge efficiency with the experimental values, as well as the optimization of the experimental variables during SG film formation, is discussed in parallel work [34].

4. Summary

In the present work, sol-gel (SG) oxide films were formed on Pt foil substrates by dip-coating from Ni, Co and mixed Ni-Co sols. After withdrawing the substrate at a constant rate, the films were dried at temperatures between 100 and 400°C for various periods of time (15 min to 1 hour). The use of more rapid substrate withdrawal rates leads to thicker films, while slower withdrawal rates produce thinner films. The average thickness of the SG films under study ranged between 60 and 800 nm.

Based on the results of TEM and ED studies, it is concluded that as-formed Ni, Co and 50:50 Ni-Co SG films are nanocrystalline oxide materials. They consist of cubic units of NiO and/or CoO (and Co_3O_4, in the case of pure Co SG films). The cubic oxide units cluster together to form crystallites which are ca. 1 to 4 nm in diameter. The crystallite size depends on the oxide composition and drying conditions. The heat treatment during SG coating preparation results in the loss of water, and the higher the drying temperature, the more compact and more crystalline are the resulting films.

It is suggested that only sites on the outer surfaces of the crystallites, with easy access to the electrolyte ions and water, participate in the redox reaction. Based on the proposed model of the SG oxide film structure, the theoretically predicted charge efficiency has been calculated to be ca. 75% for Ni and Co SG oxides and ca. 60% for 50:50 Ni-Co oxide materials. This compares well with observed efficiencies of 50–60% for both pure Ni and 50:50 Ni-Co SG oxide films, thus supporting this hypothesis. The low experimental charge efficiency observed for the pure Co SG oxide films can be attributed to the low surface area of these films, in which small crystallites may agglomerate to form clusters.

Acknowledgements

The authors gratefully acknowledge Dr. J. Ding for assistance with the TEM and ED study and Dr. R. Davidson of Surface Science Western, University of Western Ontario for obtaining the FESEM images. Financial assistance from the Department of Chemistry (University of Calgary), the Killam Trust Foundation, PanCanadian Petroleum Ltd., the Province of Alberta, ASC—Division of Analytical Chemistry, JIAS of Canada and A.S.M. International "Calgary Chapter" for the scholarship support of I. S. is gratefully acknowledged. We are also very grateful to the overall support of this research by the Natural Sciences and Engineering Research Council of Canada (NSERC).

References

1. S. KIM, D. A. TRYK, M. R. ANTONIO, R. CARR and D. A. SCHERSON, *J. Phys. Chem.* **98** (1994) 10269.
2. J. Mc BREEN, "The Ni oxide electrode," in Modern Aspects of Electrochemistry, Vol. 21, edited by R. WHITE, J. BOCKRIS and B. CONWAY (Plenum Press, New York, 1990).
3. P. BARBOUX, J. M. TARASCON and F. K. SHOKOOHI, *J. Solid State Chem.* **94** (1991) 185.
4. T. MARUYAMA and S. ARAI, *J. Electrochem. Soc.* **143** (1996) 1383.
5. I. NIKOLOV, R. DARKAOUI, E. ZHECHEVA, R. STOYANOVA, N. DIMITROV and T. VITANOV, *J. Electroanal. Chem.* **429** (1997) 157.
6. L. C. SCHUMACHER, I. B. HOLZHUETER, I. R. HILL and M. J. DIGNAM, *Electrochim. Acta* **35** (1990) 975.
7. K. LIAN, S. J. THORPE and D. W. KIRK, *ibid.* **37** (1992) 2029.
8. S. I. CORDOBA-TORRESI, C. GABRIELLI, A. HUGOT-LE GOFF and R. TORRESI, *J. Electrochem. Soc.* **138** (1991) 1548.
9. S. I. CORDOBA-TORRESI, A. HUGOT-LE GOFF and S. JOIRET, *ibid.* **138** (1991) 1554.
10. M. CHIGANE and M. ISHIKAWA, *ibid.* **141** (1994) 3439.
11. N. KRASTEVA, V. FOTTY and S. ARMYANOV, *ibid.* **141** (1994) 2864.
12. J. KUPKA and A. BUDNIOK, *J. Appl. Electrochem.* **20** (1990) 1015.
13. R.-N. SINGH, M. HAMDANI, J.-F. KOENIG, G. POILLERAT, G. L. GAUTIER and P. CHARTIER, *ibid.* **20** (1990) 442.
14. K. LIAN, D. W. KIRK and S. J. THORPE, *Electrochim. Acta* **36** (1991) 537.
15. O. LEV, Z. WU, S. BHARATHI, V. GLEZER, A. MODESTOV, J. GUN, L. RABINOVICH and S. SAMPATH, *Chem. Mater.* **9** (1997) 2354.
16. U. GEORGI, E. BRENDLER, H. GORZ and G. ROEWER, *J. Sol-Gel Sci. Technol.* **8** (1997) 507.
17. G.-W. JANG, C. CHEN, R. W. GUMBS, Y. WEI and J.-M. YEH, *J. Electrochem. Soc.* **143** (1996) 2591.

18. P. P. TRZSKOMA-PAULETTE and A. NAZERI, *ibid.* **144** (1997) 1307.
19. I. SEREBRENNIKOVA and V. I. BIRSS, *ibid.* **144** (1997) 566.
20. A. SURCA, B. OREL, B. PIHLAR and P. BUKOVEC, *J. Electroanal. Chem.* **408** (1996) 83.
21. A. SURCA, B. OREL and B. PIHLAR, *J. Sol-Gel Sci. Technol.* **8** (1997) 743.
22. K.-C. LIU and M. A. ANDERSON, *J. Electrochem. Soc.* **143** (1996) 124.
23. A. SURCA, B. OREL, R. CERC-KOROSEC, P. BUKOVEC and B. PIHLAR, *J. Electroanal. Chem.* **433** (1997) 57.
24. F. SVEGL, B. OREL, M. G. HUTCHINS and K. KALCHER, *J. Electrochem. Soc.* **143** (1996) 1532.
25. M. EL BAYDI, G. POILLERAT, J.-L. REHSPRINGER, J. L. GAUTIER, J.-F. KOENIG and P. CHARTIER, *J. Solid State Chem.* **109** (1994) 281.
26. E. C. BARRERA, T. G. VIVEROS and U. MORALES, *WREC* (1996) 733.
27. G. SPINOLO, S. ARDIZZONE and S. TRASATTI, *J. Electroanal. Chem.* **423** (1997) 49.
28. F. SVEGL, B. OREL and M. HUTCHINS, *J. Sol-Gel Sci. Technol.* **8** (1997) 765.
29. S. H. CHANG, S.-G. KANG and K. H. JANG, *Bull. Korean Chem. Soc.* **18** (1997) 61.
30. R. MONACI, A. MUSINU, G. PICCALUGA and G. PINNA, *Mater. Sci. Forum* **195** (1995) 1.
31. M. EL BAYDI, S. K. TIWARI, R. N. SINGH, J.-L. REHSPRINGER, P. CHARTIER, J. F. KOENIG and G. POILLERAT, *J. Solid State Chem.* **116** (1995) 157.
32. F. SVEGL, B. OREL, P. BUKOVEC, K. KALCHER and M. G. HUTCHINS, *J. Electroanal. Chem.* **418** (1996) 53.
33. I. SEREBRENNIKOVA, Ph.D. Thesis, University of Calgary 1999.
34. I. SEREBRENNIKOVA and V. I. BIRSS, under review in the *J. Electrochem. Soc.*
35. F. H. MOSER and N. R. LYNAM, U. S. Patent 4,959,247 (1990).
36. C. J. BRINKER and G. W. SCHERER, "SG Science" (Academic Press, San Diego, 1990).
37. A. CO, I. SEREBRENNIKOVA and V. I. BIRSS, in preparation.
38. V. C. WILLIAMS, Ph. D. Thesis, St. Catherine's College, Oxford, 1998.
39. JCPDS—International Centre for diffraction data (1996), File 01-1239.
40. JCPDS—International Centre for diffraction data (1996), File 04-0835.
41. JCPDS—International Centre for diffraction data (1996), File 02-1189.
42. JCPDS—International Centre for diffraction data (1996), File 02-1079.
43. JCPDS—International Centre for diffraction data (1996), File 42-1300.
44. JCPDS—International Centre for diffraction data (1996), File 02-1216.
45. JCPDS—International Centre for diffraction data (1996), File 44-1159.
46. JCPDS—International Centre for diffraction data (1996), File 09-0418.
47. JCPDS—International Centre for diffraction data (1996), File 09-0402.
48. JCPDS—International Centre for diffraction data (1996), File 02-1216.
49. JCPDS—International Centre for diffraction data (1996), File 09-0418.
50. JCPDS-International Centre for diffraction data (1996), File 43-1003.
51. H. GLEITER, in "Science of Advanced Materials," edited by H. Wedersich and M. Meshii (ASM International, Ohio, 1988) p. 203.
52. Z. XUPING and C. GUOPING, *Thin Solid Films* **298** (1997) 53.
53. C. NATARAJAN, H. MATSUMOTO and G. NOGAMI, *J. Electrochem. Soc.* **144** (1997) 121.
54. R. P. SIMPRAGA, *J. Electroanal. Chem.* **355** (1993) 79.

Received 8 November 2000
and accepted 17 April 2001